THE JOURNAL OF PHYSICAL CHEMISTRY B

Article

pubs.acs.org/JPCB

Electroporation Threshold of POPC Lipid Bilayers with Incorporated Polyoxyethylene Glycol ($C_{12}E_8$)

Andraž Polak,[†] Aljaž Velikonja,[†,‡] Peter Kramar,[†] Mounir Tarek,*[,§,∥] and Damijan Miklavčič*[,†]

[†]University of Ljubljana, Faculty of Electrical Engineering, Tržaška cesta 25, SI-1000 Ljubljana, Slovenia

[‡]SMARTEH Research and Development of Electronic Controlling and Regulating Systems, Poljubinj 114, SI-5220 Tolmin, Slovenia

[§]Université de Lorraine, UMR 7565, F-54506 Vandoeuvre-lès-Nancy, France

[∥]CNRS, UMR 7565, F-54506 Vandoeuvre-lès-Nancy, France

ABSTRACT: Electroporation relates to a phenomenon in which cell membranes are permeabilized after being exposed to high electric fields. On the molecular level, the mechanism is not yet fully elucidated, although a considerable body of experiments and molecular dynamic (MD) simulations were performed on model membranes. Here we present the results of a combined theoretical and experimental investigation of electroporation of palmitoy-oleoyl-phosphatidylcholine (POPC) bilayers with incorporated polyoxyethylene glycol ($C_{12}E_8$) surfactants. The experimental results show a slight increase of the capacitance and a 22% decrease of the voltage breakdown upon addition of $C_{12}E_8$ to pure POPC bilayers. These results were qualitatively confirmed by the MD simulations. They later revealed that the polyoxyethylene glycol molecules play a major role in the formation of hydrophilic pores in the bilayers above the electroporation threshold. The headgroup moieties of the latter are indeed embedded in the interior of the bilayer, which favors formation of water wires that protrude into its hydrophobic core. When the water wires extend across the whole bilayer, they form channels stabilized by the $C_{12}E_8$ head groups. These hydrophilic channels can transport ions across the membrane without the need of major lipid head-group rearrangements.

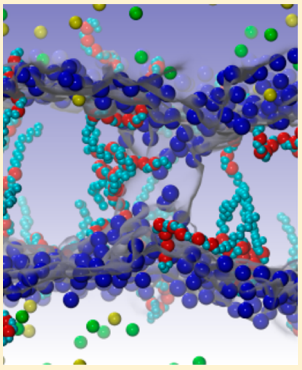

INTRODUCTION

Electroporation relates to a phenomenon in which cell membranes are permeabilized after being exposed to high electric fields.[1] Cell electroporation is used in several fields like biology, biotechnology, food processing, and medicine.[2] It is considered reversible if cells recover their initial state after the electric field is switched off. On the contrary, electroporation is considered irreversible if it leads to cell death. Among nowadays applications of electroporation based techniques, we can list electrochemotherapy,[3] transdermal drug delivery,[4] gene therapy,[5] water cleaning,[6] food processing,[7] and tissue ablation.[8] In biotechnology, protocols using electroporation to trigger drug release from smart-liposome-based nanocarriers are being devised as well.[9] Experimental evidence suggests that the effect of an applied external electric field to cells is to produce aqueous pores specifically in their membrane lipid bilayer. Information about the sequence of events describing the electroporation phenomenon can be gathered from measurements of electrical currents through planar lipid bilayers and from the characterization of molecular transport of molecules into (or out of) cells subjected to electric field pulses. The application of electrical pulses induces rearrangements of the membrane components (water and lipids) that ultimately lead to the formation of transmembrane pores, the presence of which increases substantially ionic and molecular transport through the otherwise impermeable membrane.[5,10−12] To provide a molecular level characterization of the phenomena, several groups have resorted over a decade ago to atomistic simulations that have proven to be effective in providing insights into both the structure and the dynamics of model lipid membranes.[13] Molecular dynamics (MD) simulations have hence provided so far the most informative molecular model of electroporation processes of lipid bilayers.

Electroporation may be triggered by applying long (microseconds) low magnitude (kV/m) electric pulses. These pulses cause accumulation of charges at cell boundaries over a charging time in the order of 100s of ns.[14] As the cell membranes behave as capacitors, this charge accumulation gives rise to a transmembrane potential U_t. Molecular dynamics *in silico* protocols have so far been developed to mimic the effect of such low magnitude microsecond electric pulses (μsEP) on planar bilayers by imposing a net charge imbalance across the zwitterionic membranes.[15,16] An ionic transmembrane charge imbalance was introduced 10 years ago for the first time where a double bilayer setup was utilized to impose a voltage across a bilayer.[16] The next year, this setup was used to model electroporation phenomena.[23] We have later employed the ionic transmembrane charge imbalance without using the two bilayers in a simulation box.[19]

The electric pulses induce the formation of hydrophilic pores in which transmembrane water columns created above an electroporation threshold are stabilized by lipid head groups.

Received: September 27, 2014
Revised: December 13, 2014
Published: December 15, 2014

DOI: 10.1021/jp509789m
J. Phys. Chem. B 2015, 119, 192−200

This stabilization is a crucial step in the so-called electropore life cycle[17] and is considered a prerequisite for ion conduction as reported by most MD simulation studies so far.[16,18−21]

Most of these studies have been performed on simple zwitterionic lipids (phosphatidyl choline (PC) head groups) at the exception of a few that considered also a small fraction of negatively charged lipids to study their externalization.[22] It was shown that applying a large transmembrane voltage induces the formation of hydrophilic pores, in which transmembrane water columns are stabilized by the head groups of the lipid bilayer. This step in the so-called electropore life cycle[17] is a prerequisite for ion conduction.[18,20,21,23,24] Recently,[25,26] we have found that, for some particular lipids, pores formed in bilayers subject to high transmembrane voltage may not have the same morphology as the commonly created hydrophilic pores. For lipids from archaea, for instance,[25] we did not observe rearrangement of lipid headgroups to stabilize the water wires created in the membrane. The cell membranes of these types of archaea have however a unique composition, a high chemical and a high physical stability[27−29] compared to simple phosphatidyl choline (PC) lipids, as they carry head groups formed by sugar moieties, ether linkages instead of ester linkages between the headgroup and the carbonyl region, and methyl branches in the lipid tails.[30] These properties appear not only to increase the stability of these bilayers to electrical stress manifested by the increase of the electroporation threshold but change also the morphology of the pores. We have found a similar pore behavior for bilayers containing cholesterol.[31] For specific bilayers such as those composed by POPS, a negatively charged lipid, we also recently found that pores created above an electroporation threshold are not stabilized by the lipid head groups.[26] Overall, these studies indicate that the electroporation process is modulated by the nature of the lipids in the bilayer and may be different from what was recently assumed. We are here revealing that pores formed during electroporation of "real" membranes made of a complex mixture of lipids, cholesterol, sugar, and other molecules may take various shapes.

The lipid composition is also known to modulate significantly the electroporation thresholds, i.e., the voltage required to break down a bilayer: several experimental studies characterized the impact of cholesterol contents, for instance, on the electroporation of simple lipid bilayers.[32−35] Most of the authors reported its stabilizing effect, as was later also found in MD simulation studies.[31,36] However, this seems to not be a universal behavior: in the case of diphytanoyl-glycerophosphocholine (DPhPC), a lipid of which the saturated hydrocarbon chains are functionalized with methyl groups, cholesterol was found to slightly decrease the electroporation threshold.[37] Electroporation thresholds were also shown to decrease upon addition of DPPC simple lipids to archaea based membrane composition.[25]

Other less studied additives that change lipid bilayer properties as well are surfactants. Troiano et al. studied the effects of incorporating polyoxyethylene glycol (i.e., $C_{12}E_8$) into the POPC bilayers.[38] They showed that the voltage breakdown of planar mixed lipid bilayers decreases as the surfactant concentration increases. Consistent with Troiano's observations, Kandušer et al. found that incorporation of $C_{12}E_8$ into the membranes of (DC3F) cell lines lowers the irreversible electroporation threshold.[39] Polyoxyethylene glycol surfactants have peculiar properties, in particular the size of their hydrophilic headgroup (see below). Even under normal conditions, their behavior in lipid membranes is quite distinct from that of other additives, e.g., cholesterol, since they have specific conformations, mobility, and interactions with the solvent and the ions present at the lipid−water interface. What role such properties play in the modulation of the electric stability of bilayers containing such a surfactant and to what extent pores that may form in the bilayer have also specific properties remain unknown.

In our present paper, we studied in particular planar POPC lipid bilayers containing the $C_{12}E_8$ surfactant. The techniques of planar lipid bilayer formation were developed over the last 50 years.[40−43] Their electrical properties, e.g., the capacitance, resistance, and voltage breakdown (electroporation threshold), can be measured in situ by voltage clamp, current clamp, and others special methods.[44] These properties obtained in experiments were then compared to results from atomistic simulations from which a further characterization of the electroporation phenomenon is presented.

MATERIALS AND METHODS

Experimental Section. Experiments under current-controlled conditions (i.e., current clamp) were performed using a measurement system described in detail elsewhere.[45] Briefly, the system allows one to estimate the capacitance using an LCR meter and it measures the voltage breakdown by applying a linearly rising current signal. The chamber where planar lipid bilayers are formed consists of two 5.3 cm^3 reservoirs made of Teflon. Between the two compartments, a thin Teflon sheet with a round aperture (~105 μm diameter) is inserted. Planar lipid bilayers were formed by the Montal−Mueller method.[43] We studied bilayers prepared from 1-pamitoyl 2-oleoylphosphatidylcholine (POPC) (AvantiPolar-Lipids, Alabaster, AL). The lipid powder was dissolved in a 9:1 hexane/ethanol solution 10 mg/mL. A 3:7 mixture of hexadecane and pentane was used for torus formation. The salt solution consisted of 0.1 M KCl and 0.01 M HEPES in the same proportion. Also, 1 M NaOH was added to obtain pH 7.4. For the bilayer with a surfactant content, we followed the protocol set by Troiano et al.:[38] 15 μL of $C_{12}E_8$ solution at 100 times the desired concentration (1 mM) was injected into one of the compartments of the chamber, which contained 1.5 mL of solution at a height just below the aperture.

All together, 42 POPC planar lipid bilayers and 42 POPC planar lipid bilayers with $C_{12}E_8$ incorporated were formed. The measuring protocols consisted of two sets of data: the capacitance measurement and the lipid bilayer voltage breakdown measurement. The capacitance was measured using an LCR meter (Agilent 4284A, USA) and a sinusoidal signal with an amplitude of 0.025 V and a frequency of 1 kHz. The capacitance was normalized to the surface area of the bilayer, providing therefore the specific capacitance (C_{sp}). The voltage breakdown (U_{br}) was determined for each lipid bilayer by applying linear rising current signals of slope 300 μA/s. U_{br} was defined as the voltage at which a voltage drop due to the lipid bilayer rupture was detected. All the measurements were done at room temperature (25 ± 1 °C).

Molecular Dynamics Simulations. In this study, we considered hydrated POPC bilayers with incorporated $C_{12}E_8$ (Figure 1). The molecular dynamics (MD) simulations presented here were carried out using NAMD.[46] The systems were examined at constant pressure and constant temperature (NPT) or at constant volume and constant temperature (NVT) employing Langevin dynamics and the Langevin piston method. NPT conditions were used to equilibrate the lipid

DOI: 10.1021/jp509789m
J. Phys. Chem. B 2015, 119, 192−200

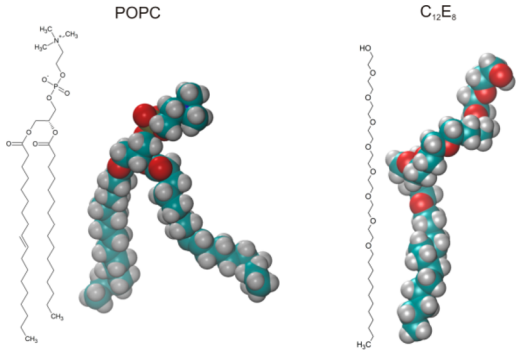

Figure 1. Representation of the structure and models of the POPC and $C_{12}E_8$ molecules. Configuration taken from the simulation of the POPC bilayer with $C_{12}E_8$ incorporated (red, oxygen; cyan, carbon; gray, hydrogen).

membranes and the NVT conditions were used to study electroporation, where the transmembrane voltage was applied using a charge imbalance method. The time step for integrating the equations of motion was set at 2.0 fs. Short- and long-range forces were calculated every one and two time steps, respectively. Bonds between hydrogen and heavy atoms were constrained to their equilibrium value. Long-range electrostatic forces were taken into account using the particle mash Ewald (PME) approach.[47]

The bilayers were built of 64 POPC lipids with 0 and 10 mol % incorporated $C_{12}E_8$ surfactant molecules in a 0.1 M KCl solution. First, simulations were performed at 50 °C (NPT) for 70 ns to relax the initial configurations. Then, we run equilibration at a lower temperature of 25 °C (NPT) for 40 ns. The final systems were constructed by replication four times of these small bilayer patches and then equilibrated at 25 °C (NPT) for 40 ns.

From the equilibrated bilayers, we calculated the average area per molecule (A_m) and the electrostatic properties of simulated lipid bilayers. The electrostatic potential profiles along the membrane normal were derived from the MD simulations using the linear Poisson equation and expressed as the double integral of the molecular charge density distributions $\rho(z)$:

$$\Phi(z) = -\varepsilon_0^{-1} \iint \rho(z'')\, dz''\, dz'$$

with z being the position of the charge in the direction along the normal to the bilayer. The dipole potential (U_d) of the bilayers is defined as the electrostatic potential difference between the middle of the bilayer (hydrophobic core) and the bulk (solvent), while the transmembrane voltage (U_t) was defined as the electrostatic potential difference between the two bulk regions surrounding the bilayer. The electron density profiles along the bilayer normal were derived directly from MD simulations.

The capacitance of each simulated membrane was estimated using the charge imbalance method.[16,19] Briefly, configurations from the equilibrated NPT runs were used to set new systems, where the simulation box size was extended in a direction perpendicular to the membrane to create air−water interfaces. For these runs, the temperature was maintained at 25 °C and the volume was maintained constant. Systems with charge imbalances of 0e, 2e, 4e, 6e, and 8e were simulated for over 1 ns each. The last 0.5 ns of simulation were used to determine the electrostatic potential distribution, from which the transmembrane voltages (U_t) were calculated. For all simulations, U_t was found in a linear correlation with q, the charge imbalance normalized to the membrane area. Accordingly, the capacitance of the bilayers was estimated as $C_{sp} = q/U_t$.

The lipid hydrocarbon chain structure is often described in terms of the deuterium order parameters. $S_{CD} = (1/2)(3\cos^2\theta - 1)$, where θ is the angle between the bilayer normal and the C−D bond of the methylene groups. The order parameter is proportional to the quadrupolar splitting in deuterium NMR experiments.

The electroporation of the lipid bilayers was induced by applying high transmembrane voltages created using the charge imbalance method. This method mimics the effect of low magnitude microsecond electric pulses.[19,20] The MD simulations of systems with 0 and 10 mol % incorporated $C_{12}E_8$ were run at several voltages. Here we report the electroporation threshold ($U_{EPthres}$) as an interval between the highest U_t at which the lipid bilayers were not electroporated in the 70 ns time scale and the lowest U_t at which pores were created in the membrane within 60 ns.

RESULTS

Experiments. We formed 42 planar lipid bilayers composed of POPC lipids and 42 POPC planar lipid bilayers with $C_{12}E_8$ incorporated. The average capacitance of the POPC planar lipid bilayer determined in this study is 0.59 μF/cm^2, which compares well to the 0.6 μF/cm^2 determined by others.[38,48,49] This capacitance increases mildly to 0.63 μF/cm^2 for the POPC planar lipid bilayers with $C_{12}E_8$ incorporated. Note that in previous studies the authors did not report that $C_{12}E_8$ has an effect to the capacitance of the POPC bilayer.[38]

Figure 2 reports a representative current and voltage trace from a single measurement in which a steady current ramp is

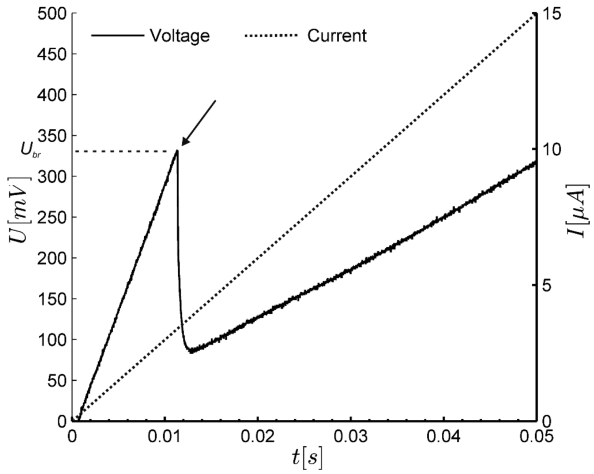

Figure 2. Voltage (U) and current (I) signals acquired in experiments using the current clamp method. The rising current is applied, and the voltage response is measured. The planar lipid bilayer is broken when the measured voltage drops (indicated by an arrow). The voltage value at which the planar lipid bilayer is broken is the voltage breakdown (U_{br}).

applied to the planar lipid bilayer. As can be seen, when the transmembrane voltage exceeds a certain value U_{br}, it abruptly collapses, indicating that the planar lipid bilayer is broken. Considering all data, incorporation of 10 mol % $C_{12}E_8$ in the POPC planar lipid bilayer lowers U_{br}. Indeed, for POPC, U_{br} amounts to 0.374 V and decreases by about 22% to 0.293 V for

DOI: 10.1021/jp509789m
J. Phys. Chem. B 2015, 119, 192−200

POPC with $C_{12}E_8$ (cf. Table 1). A Student's t test showed a statistically significant difference ($P < 0.001$) between POPC bilayers and POPC bilayers with $C_{12}E_8$ incorporated for both specific capacitance and voltage breakdown.

Table 1. Specific Capacitance (C_{esp}) and Voltage Breakdown (U_{br}) of POPC Planar Lipid Bilayers without and with $C_{12}E_8$ Incorporated in 0.1 M KCl Measured Experimentally[a]

bilayer	n	C_{esp} (μF/cm^2)	U_{br} (V)
POPC	42	0.59 ± 0.03	0.374 ± 0.046
POPC + 10 μM $C_{12}E_8$	42	0.63 ± 0.03	0.293 ± 0.044

[a]Values given are mean ± standard deviation. The number of measurements n in each experimental group is given in the second column. Specific capacitances are statistically different ($P < 0.001$), and voltage breakdowns are statistically different ($P < 0.001$). They were compared using a Student's t test.

MD Simulations. The evolution of the average area per molecule (A_m) determined from the runs shows that the systems were well equilibrated within a few tens of ns (data not shown). Quite interestingly, A_m of the POPC bilayer and of the POPC bilayers with incorporated $C_{12}E_8$ are almost the same (Table 2), indicating that within this construct (the bilayer)

Table 2. Area per Lipid (A_m), Membrane Dipole Potential (U_d), and Specific Capacitance (C_{msp}) of the POPC Bilayers with and without Incorporated Surfactant $C_{12}E_8$ in 0.1 M KCl from MD Simulations[a]

bilayer	A_m (Å^2)	U_d (V)	C_{msp} (μF/cm^2)
POPC	60.4 ± 0.7	0.68	0.88
POPC + 10 mol % $C_{12}E_8$	60.7 ± 0.9	0.66	0.97

[a]Values given are mean ± standard deviation.

$C_{12}E_8$ occupies a similar area as POPC. Using the CHARMM 36 force field, the area per lipid of pure POPC bilayers was estimated to be 64.7 ± 0.2 Å^2 at 30 °C.[50] This value is higher than the A_m calculated in our study, but here, the temperature was 25 °C. The experimental value of A_m of the POPC bilayer is 68.3 ± 1.5 Å^2 at 30 °C.[51]

There are no large differences between the POPC bilayer with and without incorporated $C_{12}E_8$ density profiles (Figure 3A). These are almost symmetrical across the plane placed in the middle of the bilayer, which means that the membranes are well equilibrated. The $C_{12}E_8$ molecules present a bimodal distribution (Figure 3B). In particular, the hydrophilic head groups of the molecules are mainly located near the glycerol lipid head groups but extend also out of the bilayer where it interacts with ions of the surrounding solution. For $C_{12}E_8$ molecules reaching out to this outer interface, we note the formation of specific configurations where, when a potassium ion from solution comes close to the hydrophilic part of $C_{12}E_8$, the latter wraps the ion (Figure 4).

The electrostatic potential profiles across the POPC bilayers with $C_{12}E_8$ incorporated were estimated from the charge distribution in the system. These analyses indicate that adding $C_{12}E_8$ into the bilayer does not significantly change the membrane dipole potential (cf. Table 1). The membrane dipole potentials derived from our MD simulations are less than 0.7 V. The dipole potential measured experimentally is ~0.363 V,[52] but other MD simulation studies also reported that the membrane dipole potential is ~0.6 V.[53]

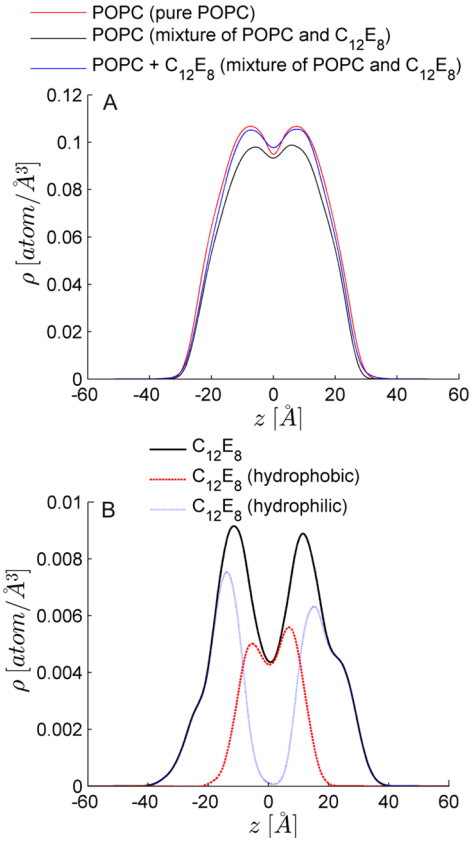

Figure 3. (A) Density profiles of lipids and $C_{12}E_8$ molecules. (B) Density profiles of $C_{12}E_8$ molecules and their hydrophobic and hydrophilic parts in the POPC bilayer.

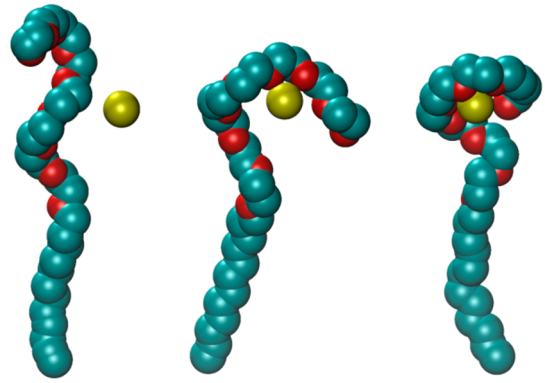

Figure 4. Snapshots of $C_{12}E_8$ when it wraps the potassium ion (red, oxygen; cyan, carbon; yellow, potassium).

The lipid bilayers were subjected to transmembrane voltages (U_t) created by means of the charge imbalance method. This allowed us to estimate first the capacitances of the POPC bilayers with 0 and 10 mol % incorporated $C_{12}E_8$. The values obtained were 0.88 and 0.97 μF/cm^2, respectively (Table 1). These values are higher than those measured experimentally (0.6 μF/cm^2)[38] but in the range of other values estimated by means of molecular dynamic simulations.[19] Note that these data obtained from simulations reproduced a slight increase in capacitance between the pure POPC bilayer and the POPC bilayer with $C_{12}E_8$ incorporated determined experimentally.

The deuterium ordered parameters are shown in Figure 5. The zero value means that the C−D (C−H) bond vectors are

DOI: 10.1021/jp509789m
J. Phys. Chem. B 2015, 119, 192−200

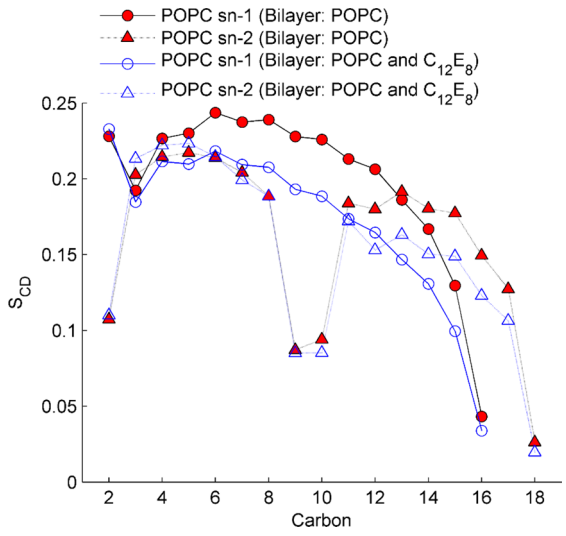

Figure 5. Order parameters (S_{CD}) for the sn-1 and sn-2 chains of POPC lipid in the bilayers composed of pure POPC and POPC with incorporated $C_{12}E_8$.

randomly oriented; on the other hand, the value 1 means that the C−D bond vector is parallel to the normal of the bilayer. The sn-1 chain of the POPC membrane is more ordered in pure POPC bilayers than in the POPC bilayer with incorporated $C_{12}E_8$. The same is noted for the sn-2 chains for carbons located at the end tail, in particular those located below the POPC double bond.

We then performed additional simulations at higher transmembrane voltages to trigger electroporation of the lipid bilayers under investigation (cf. Table 3). In the cases where test voltages did not lead to the creation of a pore (for simulation times less than 70 ns), we concluded that the electroporation threshold $U_{EPthres}$ is higher. We have determined the electroporation threshold as lying between the U_t values where the pores have not occurred and the U_t values where we observed the pore creation. The $U_{EPthres}$ intervals found for POPC bilayers with 0 and 10 mol % incorporated $C_{12}E_8$ are 1.9−2.3 and 0.7−1.1 V, respectively. The $U_{EPthres}$ value of the POPC lipid bilayer with incorporated $C_{12}E_8$ is about 50% lower than the $U_{EPthres}$ value of the pure POPC bilayer (more than 0.8 V lower). This is in qualitative agreement with the experimental data, where U_{br} of POPC bilayers with incorporated $C_{12}E_8$ was 22% lower than U_{br} of pure POPC bilayers and in agreement with the Troiano et al. study.[38]

The pore formation in pure POPC bilayers under high transmembrane voltage was studied and was described before.[13,17,20] We observed here a similar behavior. Electroporation starts by protrusion of water molecules into the hydrophobic region to form water fingers. Water fingers either extend or coalesce with others forming from the opposite side to form a water wire that extends through the bilayer (hydrophobic pore) (Figure 6B). As these water columns become larger, the lipids from both leaflets migrate into the interior of the bilayer to stabilize them, thus forming hydrophilic pores. If the voltage is maintained, the hydrophilic pores conduct the ions present in the solution (Figure 6C).

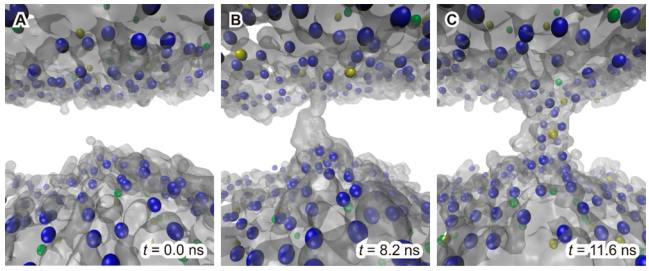

Figure 6. Electroporation of the POPC bilayer at U_t = 2.3 V (snapshots at successive times after imposing a transmembrane voltage above the threshold): (A) initial configuration, (B) formation of a water wire, and (C) formation of a conducting "hydrophobic" pore (blue, phosphorus atom; yellow, potassium ion; green, chloride ion; water, gray surface).

POPC bilayers with $C_{12}E_8$ incorporated at the concentration considered in our study have a peculiar way of forming pores when subjected to high transmembrane voltages. Initially, the hydrophobic and hydrophilic segments of $C_{12}E_8$ are mostly aligned with the hydrophobic and hydrophilic segments of the POPC lipids (Figure 7A). Some $C_{12}E_8$ molecules also form small clusters with their hydrophilic part embedded in the interior of the bilayer core. These clusters appear to favor the formation of the water wires that are dragged into the bilayer by $C_{12}E_8$ molecules. When the water wire extends across the whole lipid bilayer (Figure 7C), it forms water channels stabilized by the $C_{12}E_8$ head groups. Thus, the stabilized pore can now transport ions across the membrane (Figure 7E). It is only much later if the transmembrane voltage is maintained that a few lipid molecules migrate into the interior of the POPC bilayer and stabilize the pore even further (Figure 7F).

Table 3. Electric Characteristics of the POPC Bilayers with Incorporated Surfactant $C_{12}E_8$ under Various Transmembrane Voltages Created by a Net Charge Imbalance[a]

bilayer	Q_{im} (e)	U_t (V)	t_{sim} (ns)	t_{water} (ns)	t_{ion} (ns)	pore observed
POPC	8	1.9	71			no
	10	2.3	105	41.1	42.6	yes
POPC + 10 mol % $C_{12}E_8$	4	0.7	80			no
	6	1.1	37	29.7		yes
	8	1.5	68	47.9	51.6	yes
	10	1.9	78	14.7	15.8	yes
	12	2.3	10	2.3	3.3	yes

[a] Q_{im}, charge imbalance; U_t, transmembrane voltage; t_{sim}, simulation time; t_{water}, time when the first water wire is formed; t_{ion}, time when the first ion goes through the pore.

DOI: 10.1021/jp509789m
J. Phys. Chem. B 2015, 119, 192−200

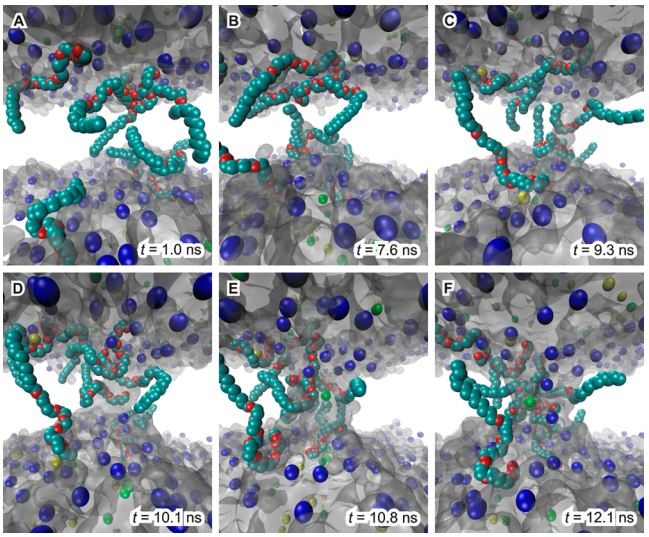

Figure 7. Electroporation of the POPC bilayer with incorporated $C_{12}E_8$ at U_t = 1.5 V (snapshots at successive times after imposing a transmembrane voltage above the threshold): (A) initial configuration, (B) $C_{12}E_8$ molecules go into the bilayer, (C) formation of a water channel stabilized by $C_{12}E_8$, (D) wider water channel stabilized by $C_{12}E_8$, (E) conducting water channel stabilized by $C_{12}E_8$, and (F) conducting water channel stabilized by $C_{12}E_8$ and POPC lipids. (blue, phosphorus atom; yellow, potassium ion; green, chloride ion; water, gray surface; cyan and red, $C_{12}E_8$ molecules).

DISCUSSION

In this study, we focused on studying the change of the properties of POPC bilayers, due to addition and incorporation of $C_{12}E_8$ experimentally and using MD simulations. The experiments on planar lipid bilayers showed that $C_{12}E_8$ has only a very mild effect on the lipid bilayer capacitance. The capacitances of the formed bilayers are in the range of those reported in other studies.[38] Our MD results show however that $C_{12}E_8$ molecules increase sensibly the capacitance of the POPC bilayer. Note here that the concentration of $C_{12}E_8$ molecules incorporated in the POPC bilayers in the simulations cannot be directly related to the one in experiments. Indeed, experimentally, only the overall initial bulk concentration of $C_{12}E_8$ is known, and it is very difficult to estimate the surfactant to lipid ratio in the formed bilayers. In the simulations, on the other hand, we have considered $C_{12}E_8$ molecules fully incorporated in the bilayer. Therefore, one can make only a qualitative comparison between the experiments and the results from simulations about the effect of the surfactant on the properties of the POPC bilayer.

The MD simulations allow one to investigate how, at the molecular level, the POPC and the incorporated $C_{12}E_8$ molecules are distributed in the equilibrated bilayer. $C_{12}E_8$ are mostly oriented with their hydrophobic tail inside the lipid bilayer and their hydrophilic moieties located in headgroup region and out of the lipid/water interface. The simulations indicated however that, often, $C_{12}E_8$ hydrophilic head groups also partition in the hydrophobic region, though no specific flip-flop of $C_{12}E_8$ was observed, perhaps due to a too short time of simulation. Experimentally, the latter was shown to occur on the seconds time scale.[54,55] Quite noticeably, in the simulations, one could detect penetration of the $C_{12}E_8$ headgroup, wrapping potassium ions toward the lipid inner core.

The voltage breakdown of POPC bilayers in experiments was measured using the current clamp method.[45] The absolute values of breakdown voltages, therefore, cannot be directly compared to those determined in other studies, due to their dependence on the shape and nature of the applied signal.[38] However, when comparing POPC bilayers with the POPC bilayers with $C_{12}E_8$ incorporated, a reduction of voltage breakdown by 22% at planar lipid bilayers was observed. It was found that 0.490 V is the minimum value to break the POPC planar lipid bilayer. Trioano et al. applied voltage pulses to the planar lipid bilayers ranging from 10 μs to 10 s. Pure POPC bilayers had breakdown voltages ranging from 0.450 to 0.167 V. POPC bilayers with incorporated $C_{12}E_8$ had 15, 26, and 33% lower voltage breakdown upon the addition of 0.1, 1, and 10 μM $C_{12}E_8$, respectively.

The decrease of the electroporation threshold estimated from the MD simulations is qualitatively consistent with experiments. The threshold estimated from the MD simulations namely decreases from 1.9−2.3 V for the pure POPC bilayer to 0.7−1.1 V, in the presence of $C_{12}E_8$. We investigated further the morphologies of the pores formed in the systems containing the surfactant. We found that the latter have a topology that is distinct from that of pores forming in pure POPC bilayers. Consistent with previous simulations,[13,17,20] in the PC pure bilayers, the pores start forming with water wires and then expand to form conducting hydrophilic pores stabilized by the PC head groups that migrate toward the lipid hydrophobic core. Note that it has been reported that for some bilayers, such as those formed by archaeal lipids, water wires may form conducting hydrophobic pores that are not stabilized by rearrangement of the lipids.[25] In POPC bilayers containing the polyoxyethylene glycol surfactant, probably because of their higher mobility, $C_{12}E_8$ molecules appear to immediately stabilize the hydrophilic water column, ensuring that the pore conducts ions. Eventually, the pores are further stabilized by lipid head groups, which migrate into the bilayer core. Hence, the present study indicates that $C_{12}E_8$ plays an important role in forming the conducting pore through the POPC lipid bilayer. Gurtovenko and Lyulina studied recently the electroporation of bilayers composed of PC and PE lipid monolayers. The electric-field-induced water-filled pore occurs mainly on the PC side, suggesting also that the structure of the molecules forming the bilayers has a strong effect on the electroporation process.[56] When a small surfactant is present, the scenario can be even more complex. This is the case for dimethylsulfoxide (DMSO) that incorporates into the lipid/water interfacial membrane region as recently shown. Quite interestingly, a similar morphology of the pores created above a voltage threshold was observed in DOPC membranes under the effect of DMSO.[57]

In order to investigate the reason for changes in the electroporation threshold as $C_{12}E_8$ is added to the POPC lipid bilayers, we have estimated the dipole potential across the lipid bilayer from MD simulations. The latter provides a direct estimate of the local electric field present at the lipid/water interface and might have an effect on the electroporation threshold, since it modulates the forces applied on the dipole of the interfacial water molecules.[58] The data at hand shows that the dipole potential at the concentrations investigated here does not change drastically when the surfactant is present.

In light of recent findings,[25] we have also estimated the local pressure profiles along z,[59] the bilayer normal for the two systems studied here. Namely, we have recently proposed that

DOI: 10.1021/jp509789m
J. Phys. Chem. B 2015, 119, 192−200

the lateral pressure in the hydrophobic region of lipid bilayers has an effect on the electroporation threshold.[25,30] The pressure profiles were calculated on the fly[46] from simulations performed at constant temperature and pressure as $p(z) = (1/\Delta V)[\sum_i \mathbf{m}_i\mathbf{v}_i \otimes \mathbf{v}_i - \sum_{i<j} \mathbf{F}_{ij} \otimes \mathbf{r}_{ij} f(z, z_i, z_j)]$, where $p(z)$ is the local pressure tensor in the slab centered on the coordinate z, the sum over the kinetic term running over all atoms in the slab, and $f(z, z_i, z_j)$ is a weighting function. In lipid bilayers, the pressure profiles arise due to the amphipathic nature of the lipids composing it: the hydrophilic head groups are squeezed together to prevent exposure of the hydrophobic tails to the solvent, leading to a negative lateral pressure, while the attractive dispersion forces and entropic repulsion between the lipid tails results mainly in a positive lateral pressure. Here, the comparison of the pressure profiles of POPC and POPC bilayers containing $C_{12}E_8$ (Figure 8) shows only a mild decrease for the latter in the upper region of the hydrophobic tails.

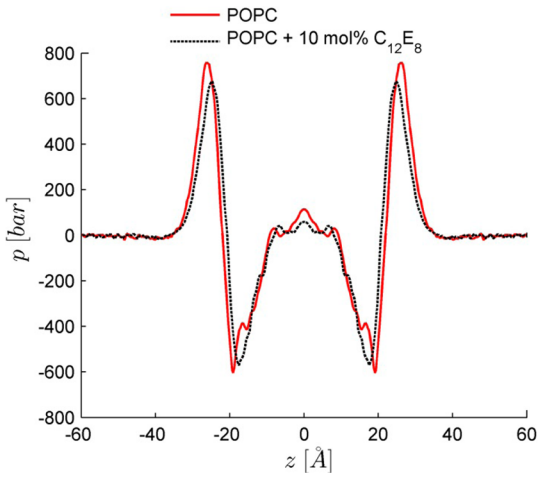

Figure 8. Pressure profile of the POPC bilayer and the POPC bilayer with incorporated 10 mol % $C_{12}E_8$.

The water permeability or diffusion toward the interior of lipid bilayers is the very initial and key step in membrane electroporation.[21,60] A significant change in the lateral pressure in the hydrophobic core of the bilayers has an effect on $U_{EPthres}$. Here, the analyses show however that the change in the lateral pressure upon addition of the surfactant is noticeable but not large. We have also investigated the effects on the lipid order parameters. The POPC order parameters for both acyl chains are lower for bilayers with incorporated $C_{12}E_8$. Similar observations were reported for bilayers, e.g., DPPC with incorporated DMSO,[61] and as cited above, the incorporation of DMSO into DOPC lipid membranes lowers the electroporation threshold.[57] Quite interestingly, incorporation of cholesterol in DPPC or DOPC bilayers increases the order parameters of the lipid acyl chains[36,62] and cholesterol increases the electroporation threshold (at least for DOPC or POPC bilayers).[31,36] Hence, it seems that the changes in the electroporation thresholds are somehow correlated with the changes in the order parameters of the lipid acyl chains the additives induce.

Another important factor that plays a role in the systems studied here is the presence of hydrophilic moieties within the bilayer hydrophobic core upon addition of $C_{12}E_8$ (Figure 3). One expects that such moieties increase the "hydrophilicity" of the lipid core and increase therefore the water permeability inside the hydrophobic core. Accordingly, we may posit here that specific configurations of the surfactant are at the origin and reason for the decrease of the electroporation thresholds observed experimentally and in MD simulations.

In conclusion, the present study reveals some key molecular properties of lipid bilayers incorporating the polyoxyethylene glycol ($C_{12}E_8$). Combining experiments and for the first time molecular dynamics simulations, the $C_{12}E_8$ has been found to modulate the electric stability of POPC bilayers even at low (10 mol %) concentration in the lipid bilayer. The properties of the surfactant, in particular its high mobility and the way its hydrophilic headgroup moiety changes the intrinsic properties of the host bilayer, were shown to be at the origin of such modulation. Incorporation of such a surfactant may serve to tune the electroporation threshold of liposomes, for instance, providing new routes for the design of efficient drug delivery carriers. Controlled electroporation can be indeed used to release the drug when such carriers have reached the proper location in a variety of applications or to reduce the irreversible threshold of electroporation in tissue ablation by means of nonthermal irreversible electroporation.[39,63]

AUTHOR INFORMATION

Corresponding Authors

*E-mail: mounir.tarek@univ-lorraine.fr.
*E-mail: damijan.miklavcic@fe.uni-lj.si.

Notes

The authors declare no competing financial interest.

ACKNOWLEDGMENTS

Research was conducted within the scope of the EBAM European Associated Laboratory. This work was in part supported by the Slovenian Research Agency and bilateral cooperation programs between France and Slovenia (PROTEUS). The manuscript is a result of the networking efforts of COST Action TD1104 (www.electroporation.net). Part of the calculations of the paper were performed during the Short Term Scientific Mission Grant STSM [070113-021794] to A.P. Simulations were performed using HPC resources from GENCI-CINES (Grant 2012-2013 [076434]). A.V. was also supported by the EuropeanSocial Fund and SMARTEH.

REFERENCES

(1) Neumann, E.; Rosenheck, K. Permeability Changes Induced by Electric Impulses in Vesicular Membranes. *J. Membr. Biol.* **1972**, *10*, 279−290.

(2) Haberl, S.; Miklavcic, D.; Sersa, G.; Frey, W.; Rubinsky, B. Cell Membrane Electroporation-Part 2: The Applications. *IEEE Electr. Insul. Mag.* **2013**, *29*, 29−37.

(3) Matthiessen, L. W.; Johannesen, H. H.; Hendel, H. W.; Moss, T.; Kamby, C.; Gehl, J. Electrochemotherapy for Large Cutaneous Recurrence of Breast Cancer: A Phase II Clinical Trial. *Acta Oncol.* **2012**, *51*, 713−721.

(4) Denet, A.-R.; Vanbever, R.; Préat, V. Skin Electroporation for Transdermal and Topical Delivery. *Adv. Drug Delivery Rev.* **2004**, *56*, 659−674.

(5) Daud, A. I.; DeConti, R. C.; Andrews, S.; Urbas, P.; Riker, A. I.; Sondak, V. K.; Munster, P. N.; Sullivan, D. M.; Ugen, K. E.; Messina, J. L.; et al. Phase I Trial of Interleukin-12 Plasmid Electroporation in Patients with Metastatic Melanoma. *J. Clin. Oncol.* **2008**, *26*, 5896−5903.

(6) Vernhes, M. .; Benichou, A.; Pernin, P.; Cabanes, P. .; Teissié, J. Elimination of Free-Living Amoebae in Fresh Water with Pulsed Electric Fields. *Water Res.* **2002**, *36*, 3429−3438.

DOI: 10.1021/jp509789m
J. Phys. Chem. B 2015, 119, 192−200

(7) Toepfl, S.; Heinz, V.; Knorr, D. High Intensity Pulsed Electric Fields Applied for Food Preservation. *Chem. Eng. Process.* **2007**, *46*, 537−546.
(8) Davalos, R. V.; Mir, L. M.; Rubinsky, B. Tissue Ablation with Irreversible Electroporation. *Ann. Biomed. Eng.* **2005**, *33*, 223−231.
(9) Elbayoumi, T. A.; Torchilin, V. P. Current Trends in Liposome Research. *Methods Mol. Biol.* **2010**, *605*, 1−27.
(10) C. Heller, L.; Heller, R. Electroporation Gene Therapy Preclinical and Clinical Trials for Melanoma. *Curr. Gene Ther.* **2010**, *10*, 312−317.
(11) Teissié, J.; Escoffre, J. M.; Paganin, A.; Chabot, S.; Bellard, E.; Wasungu, L.; Rols, M. P.; Golzio, M. Drug Delivery by Electropulsation: Recent Developments in Oncology. *Int. J. Pharm.* **2012**, *423*, 3−6.
(12) Pucihar, G.; Kotnik, T.; Miklavcic, D.; Teissié, J. Kinetics of Transmembrane Transport of Small Molecules into Electropermeabilized Cells. *Biophys. J.* **2008**, *95*, 2837−2848.
(13) Tieleman, D. P. The Molecular Basis of Electroporation. *BMC Biochem.* **2004**, *5*, 10.
(14) Kotnik, T.; Kramar, P.; Pucihar, G.; Miklavcic, D.; Tarek, M. Cell Membrane Electroporation- Part 1: The Phenomenon. *IEEE Electr. Insul. Mag.* **2012**, *28*, 14−23.
(15) Vernier, P. T.; Ziegler, M. J.; Sun, Y.; Gundersen, M. a; Tieleman, D. P. Nanopore-Facilitated, Voltage-Driven Phosphatidylserine Translocation in Lipid Bilayers–in Cells and in Silico. *Phys. Biol.* **2006**, *3*, 233−247.
(16) Sachs, J. N.; Crozier, P. S.; Woolf, T. B. Atomistic Simulations of Biologically Realistic Transmembrane Potential Gradients. *J. Chem. Phys.* **2004**, *121*, 10847−10851.
(17) Levine, Z. A.; Vernier, P. T. Life Cycle of an Electropore: Field-Dependent and Field-Independent Steps in Pore Creation and Annihilation. *J. Membr. Biol.* **2010**, *236*, 27−36.
(18) Böckmann, R. a; de Groot, B. L.; Kakorin, S.; Neumann, E.; Grubmüller, H. Kinetics, Statistics, and Energetics of Lipid Membrane Electroporation Studied by Molecular Dynamics Simulations. *Biophys. J.* **2008**, *95*, 1837−1850.
(19) Delemotte, L.; Dehez, F.; Treptow, W.; Tarek, M. Modeling Membranes under a Transmembrane Potential. *J. Phys. Chem. B* **2008**, *112*, 5547−5550.
(20) Delemotte, L.; Tarek, M. Molecular Dynamics Simulations of Lipid Membrane Electroporation. *J. Membr. Biol.* **2012**, *245*, 531−543.
(21) Kramar, P.; Delemotte, L.; Maček Lebar, A.; Kotulska, M.; Tarek, M.; Miklavčič, D. Molecular-Level Characterization of Lipid Membrane Electroporation Using Linearly Rising Current. *J. Membr. Biol.* **2012**, *245*, 651−659.
(22) Vernier, P. T.; Ziegler, M. J.; Sun, Y.; Chang, W. V.; Gundersen, M. a; Tieleman, D. P. Nanopore Formation and Phosphatidylserine Externalization in a Phospholipid Bilayer at High Transmembrane Potential. *J. Am. Chem. Soc.* **2006**, *128*, 6288−6289.
(23) Gurtovenko, A. a; Vattulainen, I. Pore Formation Coupled to Ion Transport through Lipid Membranes as Induced by Transmembrane Ionic Charge Imbalance: Atomistic Molecular Dynamics Study. *J. Am. Chem. Soc.* **2005**, *127*, 17570−17571.
(24) Gurtovenko, A. A.; Anwar, J.; Vattulainen, I. Defect-Mediated Trafficking across Cell Membranes: Insights from in Silico Modeling. *Chem. Rev.* **2010**, *110*, 6077−6103.
(25) Polak, A.; Tarek, M.; Tomšič, M.; Valant, J.; Ulrih, N. P.; Jamnik, A.; Kramar, P.; Miklavčič, D. Electroporation of Archaeal Lipid Membranes Using MD Simulations. *Bioelectrochemistry* **2014**, *100*, 18−26.
(26) Dehez, F.; Delemotte, L.; Kramar, P.; Miklavčič, D.; Tarek, M. Evidence of Conducting Hydrophobic Nanopores Across Membranes in Response to an Electric Field. *J. Phys. Chem. C* **2014**, *118*, 6752−6757.
(27) Benvegnu, T.; Brard, M.; Plusquellec, D. Archaeabacteria Bipolar Lipid Analogues: Structure, Synthesis and Lyotropic Properties. *Curr. Opin. Colloid Interface Sci.* **2004**, *8*, 469−479.
(28) Ulrih, N. P.; Gmajner, D.; Raspor, P. Structural and Physicochemical Properties of Polar Lipids from Thermophilic Archaea. *Appl. Microbiol. Biotechnol.* **2009**, *84*, 249−260.
(29) Ulrih, N. P.; Adamlje, U.; Nemec, M.; Sentjurc, M. Temperature- and pH-Induced Structural Changes in the Membrane of the Hyperthermophilic Archaeon Aeropyrum Pernix K1. *J. Membr. Biol.* **2007**, *219*, 1−8.
(30) Polak, A.; Bonhenry, D.; Dehez, F.; Kramar, P.; Miklavčič, D.; Tarek, M. On the Electroporation Thresholds of Lipid Bilayers: Molecular Dynamics Simulation Investigations. *J. Membr. Biol.* **2013**, *246*, 843−850.
(31) Casciola, M.; Bonhenry, D.; Liberti, M.; Apollonio, F.; Tarek, M. A Molecular Dynamic Study of Cholesterol Rich Lipid Membranes: Comparison of Electroporation Protocols. *Bioelectrochemistry* **2014**, *100*, 11−17.
(32) Needham, D.; Hochmuth, R. M. Electro-Mechanical Permeabilization of Lipid Vesicles. Role of Membrane Tension and Compressibility. *Biophys. J.* **1989**, *55*, 1001−1009.
(33) Neumann, E.; Kakorin, S.; Toensing, K. Fundamentals of Electroporative Delivery of Drugs and Genes. *Bioelectrochem. Bioenerg.* **1999**, *48*, 3−16.
(34) Kakorin, S.; Brinkmann, U.; Neumann, E. Cholesterol Reduces Membrane Electroporation and Electric Deformation of Small Bilayer Vesicles. *Biophys. Chem.* **2005**, *117*, 155−171.
(35) Naumowicz, M.; Figaszewski, Z. A. Pore Formation in Lipid Bilayer Membranes Made of Phosphatidylcholine and Cholesterol Followed by Means of Constant Current. *Cell Biochem. Biophys.* **2013**, *66*, 109−119.
(36) Fernández, M. L.; Marshall, G.; Sagués, F.; Reigada, R. Structural and Kinetic Molecular Dynamics Study of Electroporation in Cholesterol-Containing Bilayers. *J. Phys. Chem. B* **2010**, *114*, 6855−6865.
(37) Van Uitert, I.; Le Gac, S.; van den Berg, A. The Influence of Different Membrane Components on the Electrical Stability of Bilayer Lipid Membranes. *Biochim. Biophys. Acta* **2010**, *1798*, 21−31.
(38) Troiano, G. C.; Tung, L.; Sharma, V.; Stebe, K. J. The Reduction in Electroporation Voltages by the Addition of a Surfactant to Planar Lipid Bilayers. *Biophys. J.* **1998**, *75*, 880−888.
(39) Kandušer, M.; Fošnarič, M.; Šentjurc, M.; Kralj-Iglič, V.; Hägerstrand, H.; Iglič, A.; Miklavčič, D. Effect of Surfactant Polyoxyethylene Glycol (C12E8) on Electroporation of Cell Line DC3F. *Colloids Surf., A* **2003**, *214*, 205−217.
(40) Coronado, R.; Latorre, R. Phospholipid Bilayers Made from Monolayers on Patch-Clamp Pipettes. *Biophys. J.* **1983**, *43*, 231−236.
(41) Funakoshi, K.; Suzuki, H.; Takeuchi, S. Lipid Bilayer Formation by Contacting Monolayers in a Microfluidic Device for Membrane Protein Analysis. *Anal. Chem.* **2006**, *78*, 8169−8174.
(42) Mueller, P.; Rudin, D. O.; Tien, H. T.; Wescott, W. C. Methods for the Formation of Single Bimolecular Lipid Membranes in Aqueous Solution. *J. Phys. Chem.* **1963**, *67*, 534−535.
(43) Montal, M.; Mueller, P. Formation of Bimolecular Membranes from Lipid Monolayers and a Study of Their Electrical Properties. *Proc. Natl. Acad. Sci. U. S. A.* **1972**, *69*, 3561−3566.
(44) Kramar, P.; Miklavčič, D.; Kotulska, M.; Maček Lebar, A. Voltage- and Current-Clamp Methods for Determination of Planar Lipid Bilayer Properties. In *Advances in Planar Lipid Bilayers and Liposomes*; Iglič, A., Ed.; Elsevier: Amsterdam, The Netherlands, 2010; Vol. *11*, pp 29−69.
(45) Polak, A.; Mulej, B.; Kramar, P. System for Measuring Planar Lipid Bilayer Properties. *J. Membr. Biol.* **2012**, *245*, 625−632.
(46) Kalé, L.; Skeel, R.; Bhandarkar, M.; Brunner, R.; Gursoy, A.; Krawetz, N.; Phillips, J.; Shinozaki, A.; Varadarajan, K.; Schulten, K. NAMD2: Greater Scalability for Parallel Molecular Dynamics. *J. Comput. Phys.* **1999**, *151*, 283−312.
(47) Essmann, U.; Perera, L.; Berkowitz, M. L.; Darden, T.; Lee, H.; Pedersen, L. G. A Smooth Particle Mesh Ewald Method. *J. Chem. Phys.* **1995**, *103*, 8577.

DOI: 10.1021/jp509789m
J. Phys. Chem. B 2015, 119, 192−200

(48) Diederich, A.; Bähr, G.; Winterhalter, M. Influence of Surface Charges on the Rupture of Black Lipid Membranes. *Phys. Rev. E* **1998**, *58*, 4883.
(49) Meier, W.; Graff, A.; Diederich, A.; Winterhalter, M. Stabilization of Planar Lipid Membranes: A Stratified Layer Approach. *Phys. Chem. Chem. Phys.* **2000**, *2*, 4559−4562.
(50) Klauda, J. B.; Venable, R. M.; Freites, J. A.; O'Connor, J. W.; Tobias, D. J.; Mondragon-Ramirez, C.; Vorobyov, I.; MacKerell, A. D.; Pastor, R. W. Update of the CHARMM All-Atom Additive Force Field for Lipids: Validation on Six Lipid Types. *J. Phys. Chem. B* **2010**, *114*, 7830−7843.
(51) Kucerka, N.; Tristram-Nagle, S.; Nagle, J. F. Structure of Fully Hydrated Fluid Phase Lipid Bilayers with Monounsaturated Chains. *J. Membr. Biol.* **2005**, *208*, 193−202.
(52) Haldar, S.; Kanaparthi, R. K.; Samanta, A.; Chattopadhyay, A. Differential Effect of Cholesterol and Its Biosynthetic Precursors on Membrane Dipole Potential. *Biophys. J.* **2012**, *102*, 1561−1569.
(53) Gurtovenko, A. a; Vattulainen, I. Calculation of the Electrostatic Potential of Lipid Bilayers from Molecular Dynamics Simulations: Methodological Issues. *J. Chem. Phys.* **2009**, *130*, 215107.
(54) Kragh-Hansen, U.; le Maire, M.; Møller, J. V. The Mechanism of Detergent Solubilization of Liposomes and Protein-Containing Membranes. *Biophys. J.* **1998**, *75*, 2932−2946.
(55) Le Maire, M.; Møller, J. V.; Champeil, P. Binding of a Nonionic Detergent to Membranes: Flip-Flop Rate and Location on the Bilayer. *Biochemistry* **1987**, *26*, 4803−4810.
(56) Gurtovenko, A. A.; Lyulina, A. S. Electroporation of Asymmetric Phospholipid Membranes. *J. Phys. Chem. B* **2014**, *118*, 9909−9918.
(57) Fernández, M. L.; Reigada, R. Effects of Dimethyl Sulfoxide on Lipid Membrane Electroporation. *J. Phys. Chem. B* **2014**, *118*, 9306−9312.
(58) Aliste, M. P.; Tieleman, D. P. Computer Simulation of Partitioning of Ten Pentapeptides Ace-WLXLL at the Cyclohexane/water and Phospholipid/water Interfaces. *BMC Biochem.* **2005**, *6*, 30.
(59) Lindahl, E.; Edholm, O. Spatial and Energetic-Entropic Decomposition of Surface Tension in Lipid Bilayers from Molecular Dynamics Simulations. *J. Chem. Phys.* **2000**, *113*, 3882.
(60) Tokman, M.; Lee, J. H.; Levine, Z. a; Ho, M.-C.; Colvin, M. E.; Vernier, P. T. Electric Field-Driven Water Dipoles: Nanoscale Architecture of Electroporation. *PLoS One* **2013**, *8*, e61111.
(61) Gurtovenko, A. A.; Anwar, J. Modulating the Structure and Properties of Cell Membranes: The Molecular Mechanism of Action of Dimethyl Sulfoxide. *J. Phys. Chem. B* **2007**, *111*, 10453−10460.
(62) Smondyrev, A. M.; Berkowitz, M. L. Structure of Dipalmitoylphosphatidylcholine/cholesterol Bilayer at Low and High Cholesterol Concentrations: Molecular Dynamics Simulation. *Biophys. J.* **1999**, *77*, 2075−2089.
(63) Yarmush, M. L.; Golberg, A.; Serša, G.; Kotnik, T.; Miklavčič, D. Electroporation-Based Technologies for Medicine: Principles, Applications, and Challenges. *Annu. Rev. Biomed. Eng.* **2014**, *16*, 295−320.

DOI: 10.1021/jp509789m
J. Phys. Chem. B 2015, 119, 192−200